Preparation and Characterization of Cellulose Triacetate from Cocoa Pod Husk

Massé Bamba,[a,*] Edja Florentin Assanvo,[b] Esaïe Kouadio Appiah Kouassi,[a] Doudjo Soro,[a] Leygnima Yaya Ouattara,[a] Kouassi Benjamin Yao,[a] Allali Patrick Drogui,[c] and Dayal Rajeshwar Tyagi [c]

The valorisation of agricultural residues into a high value-added product is necessary to respond to the global environmental concerns caused by the pollution of agricultural waste. The objective of this study was to shed light on a new value-added usage of cocoa pod husk (CPH) for the synthesis of cellulose triacetate (CTA). Alkaline treatment with sodium hydroxide (5 wt%) followed by bleaching process with (2 wt%) hydrogen peroxide was found effective for the extraction of cellulose from CPH. The percentage of cellulose obtained was 80.5% with a yield of 54%. The CTA was synthesised by a explore new way acetylation reaction in the presence of acetic acid, acetic anhydride, and sulphuric acid. The CTA obtained had a degree of substitution of 2.87 and a percentage of acetylated group of 43.8%, as determined by titration. The result of Fourier transform infrared spectroscopy showed the appearance of the stretching of the ester and the acetyl groups, indicating the formation of CTA. X-ray diffraction showed that the crystallinity index of CPH cellulose was 38.4%, while indicating the semi-crystalline nature of CTA produced. Scanning electron microscopy confirmed a change in the morphology of CTA after acetylation. X-ray energy dispersive analysis showed that the CTA was mainly composed of carbon and oxygen.

INTRODUCTION

The cocoa region in Côte d'Ivoire is one of the largest pillars of the Ivorian economy, accounting for 15% of the gross domestic product (GDP) (Gitonga Njeru 2021). Ivorian cocoa production represents 40% of the world production (Statista 2022). The cocoa beans produced are either exported or transformed into many food products (chocolate powder, cocoa butter, chocolate bars, *etc*.). As for cocoa pod husk (CPH), they are released into nature as agricultural waste. However, they represent 70% to 75% of the weight of the whole pod (Daud *et al*. 2013). Their annual production in Côte d'Ivoire is estimated at more than 6.5 million tons, which explains their abundance in agricultural areas (Ouattara *et al*. 2021). This abundance results in the proliferation of mosquitoes, as

well as other harmful insects against cocoa and surrounding areas (Kouakou *et al*. 2018). To find a solution to this problem, the valarization of CPH becomes necessary.

The CPH are lignocellulosic biomasses rich in several elements such as fibres (cellulose, lignin, hemicellulose, and pectin), minerals (especially potassium), and antioxidants (polyphenols *etc*.) (Kouakou *et al*. 2018; Lu *et al*. 2018). In view of these characteristics, the valorisation of CPH has aroused the interest in many fields including soil fertilization, food and animal chemistry, plant nutrition, treatment and disposal of waste, and the technology for thermal energy (Ouattara *et al*. 2021). Most of these uses already have been widely exploited, while others such as the production of cellulose acetate from CPH are new and deserve special attention.

Cellulose is the most abundant material on Earth (Pinto *et al*. 2022), with a natural production capacity of 10^{11} at 10^{12} tons every year; it is a main element of vegetable fibres, along with hemicellulose and lignin (Motaung and Linganiso 2018; Abu Aldam *et al*. 2020; Meereboer *et al*. 2020; Pinto *et al*. 2022). It is considered an almost inexhaustible source of raw materials for the preparation of renewable and biodegradable products. Cellulose is a highly crystalline polysaccharide and is insoluble in all common organic solvents (John and Thomas 2008; Lee *et al*. 2014). With low heat treatability and poor moisture barrier performance, its usage faces problems in food packaging and other industrial applications. (Sazali *et al*. 2019). Therefore, cellulose is transformed into cellulose ester (derived from cellulose), which is biodegradable (Vroman and Tighzert 2009).

Cellulose acetate (CA) is a transparent, flexible plastic and one of the most stable cellulose derivatives. It is well known in the industrial world and generally used in applications such as sheets for food packaging, coatings, absorbent products (nappies, surgical products), membrane filters, cigarette filters, cosmetics, *etc*. (Cheng *et al*. 2010; Nguyen *et al*. 2013; Hindi and Abohassan 2015). It is obtained by acetylating the hydroxyl groups of cellulose by reacting cellulose with acetic acid and acetic anhydride in the presence of a strong acid as a catalyst (Bikales *et al*. 1954). The average number of acetylated groups per anhydroglucose unit, called the degree of substitution, ranges from 0 (in the case of cellulose) to 3 (in the case of triacetate) (Varghese *et al*. 2020). This data is very important because it governs the solubility of CA and defines some of its properties. For example, the more the DS increases, the biodegradability decreases or stops completely. It is also mentioned in the literature that CA is soluble in certain solvents such as acetone, methyl acetate, and the higher converted fractions are soluble in dichloromethane for a DS between 2 and 2.5 (Abu Aldam *et al*. 2020). Commercial CA production uses pure cellulose extracted from wood or cotton pulp. However, given the many restrictions on the preservation and conservation of forest resources, their use is becoming increasingly limited. Thus, several other sources of cellulose such as agricultural residues continue to be studied in order to obtain adequate cellulose levels for other purposes.

Moreover, several types of agricultural residues have already been used to produce CA or CTA. Hindi and Abohassan (2015) used cellulose isolated from the date palm to produce CTA by a heterogeneous acetylation reaction. This reaction was performed with acetic anhydride as the acetyl donor for a DS of 2.9 and an acetyl group ratio of 43.9% (Shaikh *et al*. 2022). Similarly, cellulose from sugarcane bagasse was used in a heterogeneous acetylation reaction to synthesize CTA with a DS of 2.81 (To Nu *et al*. 2019). In addition, Shaikh *et al*. (2022), used cellulosic fibres of cotton, recycled writing papers, recycled newspapers, and macerated woody fibres of leucocephala to produce CTA. Its various fibres have been acetylated by heterogeneous reactions with glacial acetic

bioresources.com

acid, and acetic anhydride using sulfuric acid as a catalyst. The acetylated products were obtained in respective yields of 111%, 94%, 84%, and 73% with almost identical DS (Hindi and Abohassan 2015).

Furthermore, there are previous studies on the extraction of cellulose from agricultural residues of CPH. However, so far the production of cellulose acetate from CPH still remains new and needs to be explored. Moreover, the authors wanted to emphasize the scientific and environmental interest of the valorization of an agricultural waste that is found in large quantities in Côte d'Ivoire and in West Africa. These agricultural wastes represent an enormous source of pollution of the agricultural spaces.

Hence, the objective of this study is to explore a new way of valuing CPH for the synthesis of CTA.

EXPERIMENTAL

Materials

Fresh cocoa pod husks (CPH) used in this work came from Côte d'Ivoire (CI). Ethanol (C_2H_5OH, 96%) and sodium hydroxide (NaOH) pellets were obtained from Sigma-Aldrich. Sulfuric acid (H_2SO_4, 98%) and glacial acetic acid (CH_3COOH, 99%) used were Merck brand. Acetic anhydride (($CH_3CO)_2O$, 99%) was Scharlau brand, and hydrogen peroxide (H_2O_2) was purchased from Panreac Applichem. All chemicals and solvents used were of analytical grade and were used without further purification.

Methods

Plant biomass: Mechanical treatment of plant biomass

The CPH were collected in a cocoa plantation in the village of Lolobo located in the department of Yamoussoukro (region of the lakes) in the system latitude: 6.955980 and longitude: -5.269256. The CPH samples collected were taken to the laboratory and washed with tap water several times to remove any impurities (sand, leaf, mucilage, and other contaminants). Then they were dried in the sun for 3 days and in an electric dryer for 24 h at 60 °C. The dried product was ground in a cutter mill to obtain a powder with a particle size of 200 μm. Finally, the powder was stored in a sealed bottle for chemical analyses and for the synthesis of CTA. Figure 1 shows the CPH extraction steps.
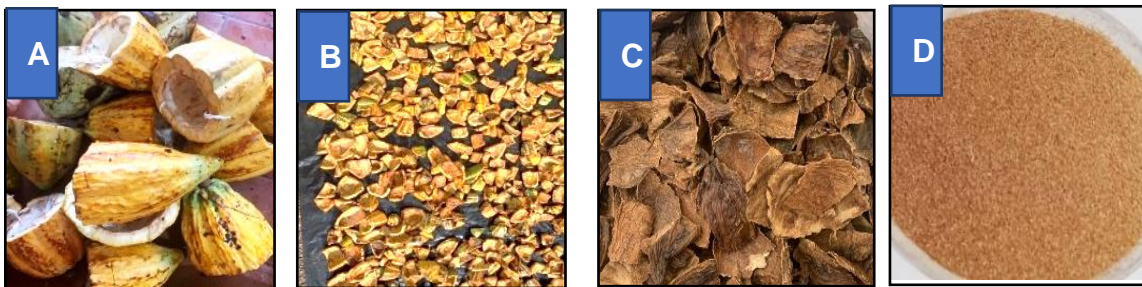

Fig. 1. Extraction steps of CPH powder: A (fresh CPH), B (sun-dried CPH), C (electrically dried CPH), and D (CPH powder).

Extraction of cellulose from cocoa pod husk (CPH)

The CPH powder was treated with boiled water and then dried at 105 °C in an oven for 24 h. The dry CPH powder was then treated with a 5% (w/v) aqueous solution of NaOH for 3 h at a temperature of 170 to 200 °C under constant mechanical stirring. The paste was then rinsed several times with distilled water until the alkali was neutralized. The solids were dried for 24 h. After that, the sample was bleached with 2% of hydrogen peroxide (H_2O_2) at pH=12 (adjusted with a concentrated solution of KOH) at 70 °C for 3 h. Subsequently, the sample was filtered, washed with distilled water to neutral pH, and dried in an oven for 6 h at 105 °C.

Synthesis of cellulose triacetate (CTA)

The preparation of CTA from CPH involved dissolving 1.0 g of dried CPH cellulose in a solution of 40 mL of glacial acetic acid with a few drops of 98% sulfuric acid as the catalyst for the reaction. The system was refluxed at a temperature of 80 to 90 °C for 30 min. After cooling, 40 mL of acetic anhydride was added to the mixture, and the system was heated again until the fibre had completely disappeared (after 15 min). A 20% aqueous solution of acetic acid was then added at the end of the reaction and the mixture is then heated at 70 °C for 10 min. After cooling (after 60 min), 50 mL of hot water (approximately 100 °C) was added slowly while stirring, when CTA precipitated. It was then filtered using Buchner funnel and the product is washed with cold water until a neutral pH. The product obtained was dried in an oven at 90 °C to a constant mass.

Analysis of the chemical composition

The chemical composition of the CPH powder and the cellulose extract of the CPH was carried out following the ASTM methods. The raw CPH powder first underwent solubilization in alternating solvents, hot water and 96% ethanol, to determine the content of extractables. Holocellulose content was determined by ASTM D1104-56 (1978), cellulose content per ASTM D1103-60 (1978), lignin content per ASTM D1106-56 (1974), and ash content per ASTM D1102-84 (2007). The hemicellulose content was obtained by subtracting between the holocellulose and cellulose contents.

Determination of % acetyl and degree of substitution DS

The degree of substitution (DS) of the CTA produced was determined by the titration method as described by Samios *et al.* (1997). For this purpose, 1 g of dry CTA was accurately weighed using an electronic balance and transferred into a 250 ml Erlenmeyer flask. Then 40 mL of a 75% (v/v) aqueous ethanol solution was added to the previous mixture. A blank test was carried out in another 250 mL Erlenmeyer flask by adding 40 mL of the 75% (v/v) ethanol solution and carrying out the rest of the procedure. Hermetically sealed Erlenmeyer flasks were heated for 30 min at 60 °C. Then, 40 mL of a solution of NaOH (0.5 N) were added to each of the Erlenmeyer flasks, and heated again at 60 °C for 30 min. The sealed flasks were then allowed to stand at room temperature for 72 h. Excess alkali was titrated with hydrogen chloride (HCl) solution (0.5 N) using phenolphthalein as indicator. An excess of 1.0 mL of HCl (0.5 N) was added, and the alkali was allowed to diffuse from the regenerated cellulose overnight. The disappearance of the pink color indicated complete neutralization of the alkali. The small excess of the acid was then titrated with NaOH (0.5 N) to the phenolphthalein endpoint. The procedure was performed in triplicate to determine the degree of acetylation and the DS using Eq. 1,

$$\% \textbf{ Acetyl} = \frac{[(A-B)N_b - (C-D)N_a)] \times 4.3}{W} \tag{1}$$

with:

$$\textbf{DS} = \frac{(3.86 \times \% \textbf{ Acetyl})}{(102.4 - \% \textbf{ Acetyl})} \tag{2}$$

where *A* is the amount of NaOH added to the sample (mL); *B* is the amount of NaOH added to the blank (mL); N_b is the normality of the NaOH solution; *C* is the amount of HCl added to the sample; *D* is the amount of HCl added to the blank (mL); N_a is the normality of the HCl solution; *W* is the sample weight (g); and 4.3 is a factor to calculate the (%) acetylation.

Characterization and Analysis Method

Fourier Transform Infrared Spectroscopy (FT-IR)

Cellulose functional groups of CPH and CTA were evaluated by Fourier transform infrared (FTIR) spectroscopy using a Jasco Model No.4700 Type A spectrometer (Chennai, India). Spectra were obtained over a range of 500 to 4000 cm^{-1} with a sweep speed of 2 mm/s. Thirty-two acquisitions were made from each spectrum at a resolution of 4 cm^{-1} and an incident angle of 45°.

X-ray diffraction analysis:

The X-ray diffractogram of the different samples was carried out on a Rigaku Miniflex (II) brand desktop diffractometer (Chennai, India) using a Ni filter ($\lambda = 1.5418$ nm) with a Cu-Kα radiation source at (35 kV and 10 mA) over an angular range between 5° and 40°. The direction-finding speed is 5°/min, and the XRD results were processed using the Joint Committee on Powder Diffraction Standards (JCPDS) software. The crystallinity index (CrI) was calculated from the Eq. 3,

$$C_r I = \frac{(I_{002} - I_{am})}{I_{002}} \times 100 \tag{3}$$

where I_{002} denotes the intensity of the maximum diffraction peaks linked to the crystalline part of the cellulose at $2\theta = 22°$ and I_{am} refers to the intensity of the minimum peaks related to the amorphous region of the cellulose $2\theta = 18°$ (Segal *et al*. 1959; Wang *et al*. 2015).

Scanning electron microscope (SEM):

The surface morphologies of CPH cellulose before and after acetylation were observed by a TESCAN field emission scanning electron microscope, CLARA model combined with EDAX (Chennai, India). The excitation energy was set at 10 KeV with a magnification of 5.00 kx.

RESULTS AND DISCUSSION

Lignocellulosic Composition of Cocoa Pod Husk and Cellulose Obtained from CPH

Cocoa pod husk

The lignocellulosic composition of CPH obtained from this study is summarized in Table 1. This table also includes results from previous studies for comparison purposes. There was heterogeneity between the results obtained and those observed in the literature (Table 1). Indeed, according to Leygnima *et al*. (2021) and Sandesh *et al*. (2020), these

bioresources.com

disparities between the results could be attributed to environmental factors, varieties of biomass, different analytical methods or the solvents used, and to the location of the materials collected.

It is also notable that the values of cellulose during this characterization were close to the results of certain authors mentioned in Table 1. On the other hand, the cellulose data were lower than the values reported by Daud *et al*. (2013) and Nazir *et al*. (2016). It should be noted that cellulose is very important because it represents the main structural component of a plant fibre. In addition, it gives strength and stability to the cell walls of the plant (Anjum *et al*. 2016).

The hemicellulose content of the CPH obtained was identical to that reported by Nazir *et al*. (2016) and Titiloye *et al*. (2013), but much lower than the data found by Asiedu *et al*. (2019) and Daud *et al*. (2013). Hemicelluloses hydrolyse more easily to sugar than cellulose and therefore fibres containing a high level of hemicellulose would be excellent for the production of fuels such as ethanol (Reddy and Yang 2005).

Regarding the lignin content in this work, it was relatively low compared to that reported by Nazir *et al*. (2016) and Titiloye *et al*. (2013), but it was high compared to the values obtained by Asiedu *et al*. (2019) and Daud *et al*. (2013). Hence the need to provide a pre-treatment in order to release the fermentable sugars (Leygnima *et al.* 2021) is evident here.

Table 1. Lignocellulosic Composition of CPH and the Results of Some Previous Studies

Cellulose (%)	Hemicellulose (%)	Lignin (%)	Extractables (%)	Reference
30.23	12.58	20.58	21.43	This work
31.68	16.97	25.62	21.57	(Leygnima *et al.* 2021)
30.41	11.97	33.96	23.66	(Titiloye *et al.* 2013)
28.25	16.75	24.16	-	(Sandesh *et al.* 2020)
23.04	38.08	18.19	-	(Asiedu *et al.* 2019)
44.69	11.15	34.82	-	(Nazir *et al.* 2016)
35.40	37.0	14.7	-	(Daud *et al.* 2013)

Cellulose isolated from cocoa pod husk

The results of the lignocellulosic composition of the cellulose isolated from CPH (CPH-Cellulose) are summarized in Table 2 and is compared to that of the raw CPH.

After extracting the cellulose, it was noted that the product obtained had a high purity in which the cellulose content had increased from 30.23% to 80.5% compared to the raw CPH. Also, it can be observed that the contents of hemicellulose and lignin had considerably decreased. This could be explained by their solubilizations during the bleaching process.

With a low concentration of H_2O_2 (2%) at pH = 12 and in the presence of NaOH, good removal of the lignin content was observed during the bleaching process. These results confirm the results of Shaikh *et al*. (2022), who showed that lignin removal was effective at low concentrations of H_2O_2 (2%) at pH = 12 (To Nu *et al*. 2019).

In this study, the yield of the CPH-cellulose obtained after the extraction process was 54%.

Table 2. Lignocellulosic Composition of Extracted Cellulose from CPH

Samples	Cellulose Extraction (Treatment)		Result				
	NaOH (%; w/v)	[H_2O_2] (%; v/v)	t (h)	Weight (a,b) (g)	C wt (%)	H_c wt (%)	L wt (%)
CPH-Cellulose	5	2	3	5.4 (b)	80.50	7.57	5.70
CPH	-	-	-	10 (a)	30.23	12.58	20.58
Weight[(a,b)]: [a] (initial weight of CPH), [b] (final weight of extracted cellulose); C (cellulose); Hc (hemicellulose); L (lignin)							

Percentage of acetyl groups and degree of substitution (DS)

The production of CTA in this study was carried out in several stages namely: activation, acetylation, hydrolysis, and drying. As a matter of fact, the activation step occurs well before acetylation in order to enlarge the surface of cellulosic fibres and reduce intermolecular hydrogen bonds (Bahmid *et al*. 2013). This facilitates the process of acetylation with acetic anhydride.

The results of the percentage of acetylated groups and the DS are summarized in Table 3. The values for the percentage of acetyl groups and the DS were 43.75% and 2.87, respectively. These results were close to the values obtained by Shaikh *et al*. (2022) and To Nu *et al.* (2019).

The DS (2.87) obtained in this study by the titration method indicates that the product obtained is cellulose triacetate (Silva *et al.* 2017; Malucelli *et al*. 2019; Shaikh *et al*. 2022). Also, note that the data presented in Table 3 indicate that the acetyl group (%) and DS value increased depending on the purity of the extracted cellulose.

Table 3. Percentage Acetyl Content and DS of Prepared Cellulose Acetate

Samples	% Acetyl	DS	Yield	Reference
CTA	43.75	2.87	62.96	This work
CTA-2	43.51	2.85	94.5	(Shaikh *et al.* 2022)
CA-1	41.68	2.65	45	(To Nu *et al.* 2019)
CA-2	43.05	2.80	51	(To Nu *et al.* 2019)
CA24	42.1	2.79	-	(Rodrigues Filho *et al.* 2008)

Fourier transform infrared (FTIR) spectroscopy

The FTIR spectra of CPH cellulose and CTA extracted from CPH are shown in Fig. 2. In the CPH cellulose spectrum, the maximum absorption band found at 3343 cm^{-1} has been attributed to the stretching of hydroxyl groups (-OH) bonded to hydrogen (Poletto *et al*. 2011; Egot and Alguno 2018; Jimat *et al*. 2019; Shaikh *et al*. 2022).

The intensity of the bands at 2907 and 1368 cm^{-1} could be attributed to stretching and straining vibrations of the (C-H) group in glucose units (Jimat *et al*. 2019). However, these inter- and intra-molecular hydrogen bonds in cellulose have a strong influence on the physical and mechanical properties of cellulose (Samuel and Adefusika 2019).

According to Poletto *et al.* (2011), the bands at 1426, 1320, and 1030 cm^{-1} can correspond respectively to the group (CH_2), to the motion of (CH_2), and to (C-O-) a group of secondary functions of alcohol and ether in the cellulosic base chain. In addition, those at 1106 cm^{-1} and 1158 cm^1 may be associated with anhydro-glucose ring and asymmetric bridge stretching of C-O-C group (Tserki *et al*. 2005; Poletto *et al*. 2011).
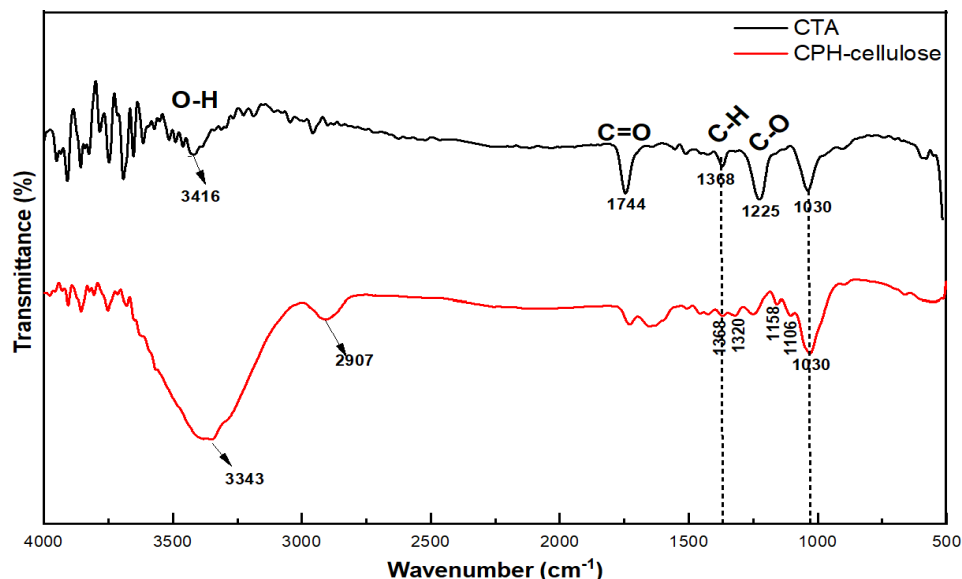
Fig. 2. FTIR spectra of CPH cellulose and cellulose triacetate

The last transmission peak observed at 895 cm^{-1} was attributed to symmetric stretching (C-O-C) of the β (1→4) glycosidic linkage. In the spectrum of cellulose isolated from CPH, the peak located in the area of 1700 cm^{-1} characteristic of the carbonyl group in hemicelluloses was absent, as well as the absence of peaks that would have indicated the presence of lignin units (1600 and 3070 cm^{-1}).

In the spectrum of CTA, the functional group (-OH) at 3416 cm^{-1} had been perfectly acetylated because it has a high value of transmission compared to that of CPH cellulose (Tristantini Budi and Yunan 2018).

Indeed, the formation of CTA could be confirmed by the peaks 1744 cm^{-1} and 1225 cm^{-1}, which correspond respectively to the stretching of the ester (C=O) and the stretching (C-O) of the acetyl group (Egot and Alguno 2018; Shaikh *et al*. 2022). Also, the bending vibrations of the methyl (C-H) in the acetate were observed at 1368 cm^{-1}. The absence of the bands at 1760,1840, and 1700 cm^{-1} showed cellulose acetate to be free of acetic anhydride and acetic acid (Heinze and Liebert 2012; Shaikh *et al*. 2022).

The presence of its four functional groups: (OH), (C=O), (C-O), and (C-H) showed that CTA produced from CPH cellulose was successfully formed in this work.

X-ray diffraction

The XRD analysis was performed to observe a change in the cellulose structure of CPH before and after acetylation, as shown in Fig. 3. Three peaks were observed on the CPH cellulose diffractogram at 2θ = 15.4°; 22.1°; and 34.5°. Its peaks are characteristic of the crystal structure of type I cellulose, as already mentioned by several authors (Matsumura *et al*. 2000; Poletto *et al*. 2011; Malucelli *et al.* 2019). After acetylation of the CPH cellulose, the three initial peaks almost disappeared on the CTA diffractogram and new maximum peaks appeared respectively at 2θ = 8.5°; 10.5°; 13.4°; 17.6; 18.3; and 21.1°. This change was due to the diffraction pattern indicating the substitution of hydroxyl groups by acetyl groups which have a larger volume along the axes (Malucelli *et al*. 2019; Morsy *et al*. 2022).
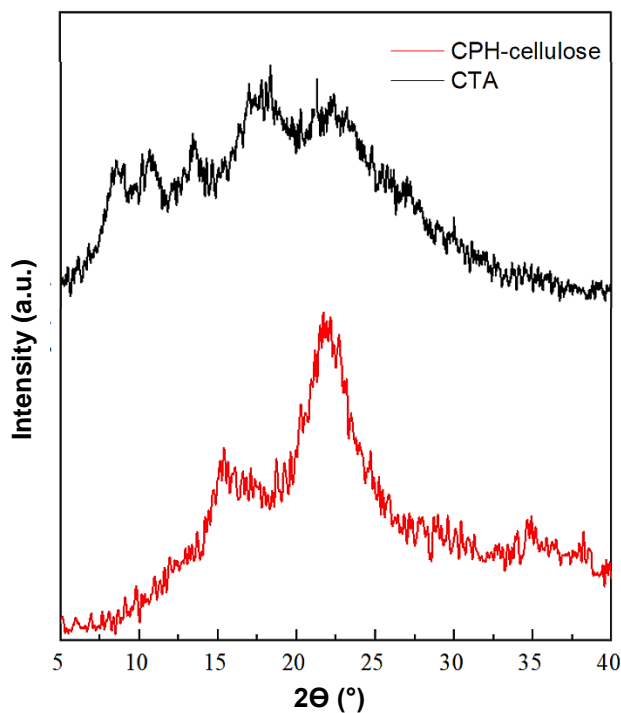
Fig. 3. X-ray diffraction patterns of cellulose extracted from CPH and cellulose triacetate (CTA)

According to previous studies (Rodrigues Filho *et al*. 2000; Yang *et al.* 2014; Malucelli *et al*. 2019), the main peak located at about 8° recorded for CTA is characteristic of semi-crystalline acetylated cellulose. At this peak, there is a generation of disorders caused by the substituent groups, resulting in an increased interfibrillar distance and a degradation of the micro fibrillar structures (Maheswari *et a*l. 2012; Malucelli *et al.* 2019). The disappearance of the various peaks after the acetylation reaction would indicate the loss of crystallinity in the acetylated sample.

The crystallinity index (CrI) of CPH cellulose was calculated using Segal's equation to be 38.4%. This result is lower than that reported by others (Maheswari *et al.* 2012; Akinjokun *et al.* 2021). This difference was attributed to the presence of residual hemicelluloses after the bleaching process, which could influence the low crystallinity of the final sample (Malucelli *et al*. 2019).

Scanning electron microscopy with energy dispersive X-ray analysis

Figure 4 shows SEM images of cellulose isolated from CPH and CTA. A difference is observed in the morphology of the two samples. The micrograph of the cellulose extracted from the CPH showed a compact surface morphology with a fairly smooth surface.

After the acetylation process, the SEM image obtained for CTA (Fig. 4b) exhibited small and large rough particles in the form of a spongy structure. This can be seen as a degradation of the structure of the cellulose triacetate sample. This deterioration could be caused by the dissolution of the CPH cellulose in the acetic anhydride. Similar micrographs have also been observed by some authors (Hamed *et al*. 2015; Hu *et al*. 2015). Moreover, Fig. 4b clearly indicates its non-fibrous nature and exhibits a morphology similar to the structure of a cellulose triacetate.
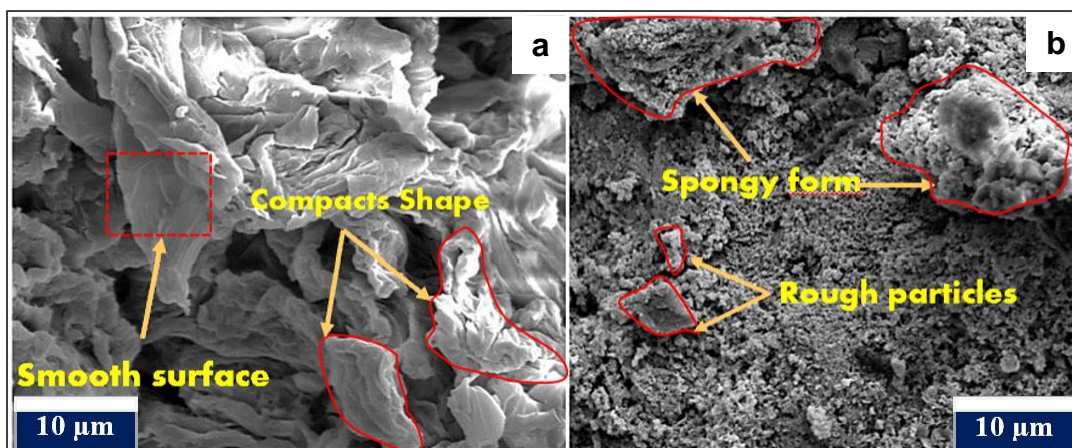
Fig. 4. SEM micrographs of (a) extracted cellulose of CPH (b) cellulose triacetate (CTA)

Energy dispersive X-ray analysis (EDAX) was used to determine the composition of chemical elements in CTA from a randomly selected point represented by a red square on the sample. The EDAX scatter spectrum of CTA is presented at Fig. 5 shows the presence of carbon (C) 87% and oxygen (O) 13%. These various results indicate that the CTA obtained represents an organic compound.
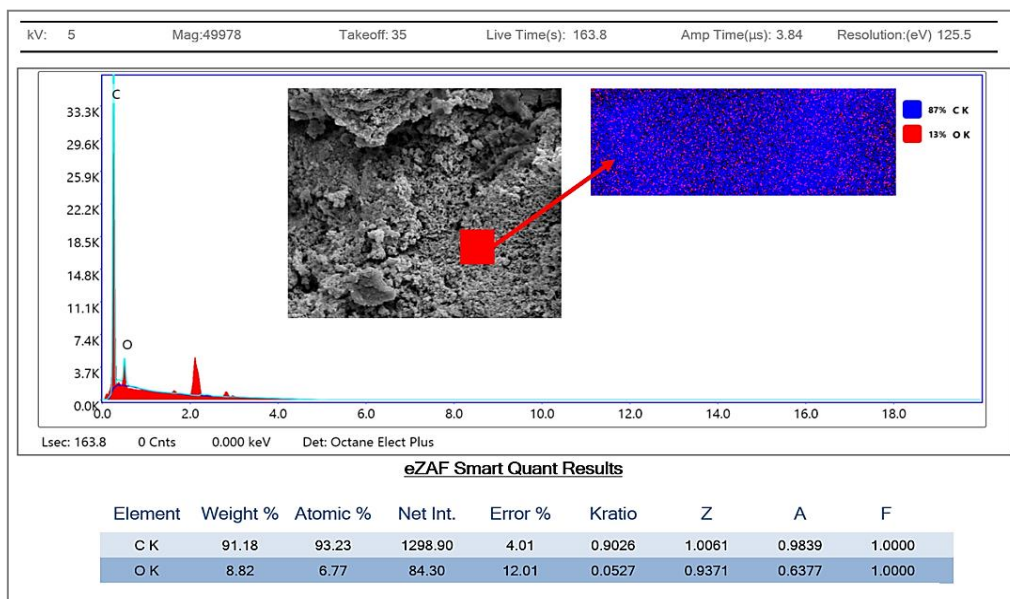

eZAF Smart Quant Results

Element	Weight %	Atomic %	Net Int.	Error %	Kratio	Z	A	F
C K	91.18	93.23	1298.90	4.01	0.9026	1.0061	0.9839	1.0000
O K	8.82	6.77	84.30	12.01	0.0527	0.9371	0.6377	1.0000

Fig. 5. EDAX of CTA sample elemental mapping

CONCLUSIONS

1. Alkaline pre-treatment of cocoa pod husk (CPH) with NaOH (5 wt%) followed by bleaching sequence with H_2O_2 (2% v/v) showed a strong improvement in the extraction of cellulose content (30.2 to 80.5%) and considerable decrease in lignin (20.6 to 5.7%) and hemicellulose (12.6 to 7.6%)

2. The cellulose extracted from CPH was modified by an acetylation reaction using acetic acid and acetic anhydride in the presence of sulfuric acid. The yield of the product obtained was 63.0% with a degree of substitution of 2.87, indicating that the product synthesized was cellulose triacetate (CTA).

3. The Fourier transform infrared (FTIR) spectrum of CPH cellulose showed an absence of the characteristic peaks of hemicelluloses at 1700 cm^{-1} and lignin at 1600 and 3070 cm^{-1}. After acetylation, the spectrum confirmed the formation of CTA through the peaks 1744 and 1225 cm^{-1} corresponding to the ester (C=O) and the acetyl (C-O) stretching.

4. The peaks in the X-ray diffraction (XRD) diffractogram of CPH cellulose were characteristic of the crystal structure of type I cellulose, while the resulting CTA had a semi-crystalline structure.

5. Scanning electron microscopy (SEM) analysis showed a change in the morphology of CPH cellulose after acetylation. The micrograph before acetylation had a compact structure and a smooth surface, whereas the one after acetylation showed small and medium sized particles in a rough and spongy form.

ACKNOWLEDGEMENTS

REFERENCES CITED

Abu Aldam, S., Dey, M., Javaid, S., Ji, Y., and Gupta, S. (2020). "On the synthesis and characterization of polylactic acid, polyhydroxyalkanoate, cellulose acetate, and their engineered blends by solvent casting," *Journal of Materials Engineering and Performance* 29(9), 5542-5556. DOI: 10.1007/s11665-020-04594-3

Akinjokun, A. I., Petrik, L. F., Ogunfowokan, A. O., Ajao, J., and Ojumu, T. V. (2021). "Isolation and characterization of nanocrystalline cellulose from cocoa pod husk (CPH) biomass wastes," *Heliyon* 7(4), article e06680. DOI: 10.1016/j.heliyon. 2021.e06680

Anjum, A., Zuber, M., Zia, K. M., Noreen, A., Anjum, M. N., and Tabasum, S. (2016). "Microbial production of polyhydroxyalkanoates (PHAs) and its copolymers: A review of recent advancements," *International Journal of Biological Macromolecules* 89, 161-174. DOI: 10.1016/j.ijbiomac.2016.04.069

Asiedu, Nana Y., Neba, Fabrice Abunde, and Ahmad Addo. (2019). "Modeling the attainable regions for catalytic oxidation of renewable biomass to specialty chemicals: Waste biomass to carboxylic acids," *South African Journal of Chemical Engineering* 30, 1-14. DOI: 10.1016/j.sajce.2019.07.003

ASTM D 1106-56. (1974). "Standard test method for lignin in wood," *American Society for Testing and Materials*, West Conshohocken, PA.

bioresources.com

ASTM D1102-84. (2007). "Standard test method for ash in wood," *American Society for Testing and Materials*, West Conshohocken, PA.

ASTM D1103-60. (1978). "Standard test methods for alpha-cellulose in wood," *American Society for Testing and Materials,* West Conshohocken, PA.

ASTM D1104-56. (1978). "Standard test method for holocellulose in wood," *American Society for Testing and Materials*, West Conshohocken, PA.

Bahmid, N., Syamsu, K., and Maddu, A. (2013). "Production of cellulose acetate from oil palm empty fruit bunches cellulose," *Chemical and Process Engineering Research* 17, 12-20.

Bikales, N. M., Segal, L., Ott, E., Spurlin, H. M., and Grafflin, M. W. (1954). *Cellulose and Cellulose Derivatives*, Wiley-Interscience.

Cheng, H. N., Dowd, M. K., Selling, G. W., and Biswas, A. (2010). "Synthesis of cellulose acetate from cotton byproducts," *Carbohydrate Polymers* 80(2), 449-452. DOI: 10.1016/j.carbpol.2009.11.048

Daud, Z., Sari, A., Kassim, A., Mohd Aripin, A., Awang, H., Zainuri, M., Hatta, M., Malaysia, H., and Pahat, B. (2013). "Chemical composition and morphological of cocoa pod husks and cassava peels for pulp and paper production," *Aust. J. Basic Appl. Sci.* 7, 406-411.

Egot, M., and Alguno, A. (2018). "Preparation and characterization of cellulose acetate from pineapple (*Ananas comosus*) leaves," *Key Engineering Materials* 772, 8-12. DOI : 10.4028/www.scientific.net/KEM.772.8

Gitonga Njeru, L. (2021). "Côte-d'Ivoire : Les déchets de cacao pour alimenter la centrale électrique à biomasse de Divo [Côte d'Ivoire: Cocoa waste to fuel the biomass power plant in Divo]," *Connectionivoirienne*.

Hamed, O. A., Jodeh, S., Al-Hajj, N., Hamed, E. M., Abo-Obeid, A., and Fouad, Y. (2015). "Cellulose acetate from biomass waste of olive industry," *Journal of Wood Science* (Springer Open) 61(1), 45-52. DOI: 10.1007/s10086-014-1442-y

Heinze, T., and Liebert, T. (2012). "10.05 Celluloses and polyoses/hemicelluloses," in: *Polymer Science: A Comprehensive Reference*, pp. 83-152. DOI: 10.1016/b978-0-444-53349-4.00255-7

Hindi, S. S. Z., and Abohassan, R. A. (2015). "Cellulose triacetate synthesis from cellulosic wastes by heterogeneous reactions," *BioResources* 10(3), 5030-5048. DOI: 10.15376/biores.10.3.5030-5048

Hu, H., Li, H., Zhang, Y., Chen, Y., Huang, Z., Huang, A., Zhu, Y., Qin, X., and Lin, B. (2015). "Green mechanical activation-assisted solid phase synthesis of cellulose esters using a co-reactant: effect of chain length of fatty acids on reaction efficiency and structure properties of products," *RSC Advances* 5, 20656-20662. DOI: 10.1039/C5RA02393A

Jimat, D., Putra, F. A., Sulaiman, S., Mohamed Azmin, N. F., and Putra, S. (2019). "Physicochemical characteristics of bionanocomposites, polycaprolactone/ starch/cocoa pod husk microfibrillated cellulose," *Journal of Advanced Research in Fluid Mechanics and Thermal Sciences* 55, 199-208.

John, M., and Thomas, S. (2008). "Biofibres and biocomposites," *Carbohydrate Polymers* 71(3), 343-364. DOI: 10.1016/j.carbpol.2007.05.040

Kouakou, E. K., Mouroufie, A. K., Kati-Coulibaly, S., Amed, C., Kouakou, F. K., KONAN, C. M., Kpan, E. S., and Bouafou, K. G. (2018). "Cocoa pod in the Ivorian plantations: Green gold neglected and bulky?" *Nutrition and Food Science International Journal* 7(2), 48-50.

Lee, H. V., Hamid, S. B. A., and Zain, S. K. (2014). "Conversion of lignocellulosic biomass to nanocellulose: structure and chemical process," *The Scientific World Journal* 2014, article e631013. DOI: 10.1155/2014/631013

Leygnima, Y., Ouattara, Y., Doudjo, S., Fanou, G., Kouadio, E., Kouassi, E., Bamba, M., Yao, K., Adouby, K., Drogui, A., and Tyagi, D. (2021). "Optimization of the autoclave-assisted alkaline delignification of cocoa (*Theobroma cacao*) pod husks using KOH to maximize reducing sugars," *BioResources* 17(1), 826-848. DOI: 10.15376/biores.17.1.826-848

Lu, F., Rodriguez-Garcia, J., Van Damme, I., Westwood, N. J., Shaw, L., Robinson, J. S., Warren, G., Chatzifragkou, A., McQueen Mason, S., Gomez, L., Faas, L., Balcombe, K., Srinivasan, C., Picchioni, F., Hadley, P., and Charalampopoulos, D. (2018). "Valorisation strategies for cocoa pod husk and its fractions," *Current Opinion in Green and Sustainable Chemistry Bioresources and Biochemicals / Biofuels and Bioenergy* 14, 80-88. DOI: 10.1016/j.cogsc.2018.07.007

Maheswari, C. U., Reddy, K. O., Muzenda, E., Guduri, B. R., and Rajulu, A. V. (2012). "Extraction and characterization of cellulose microfibrils from agricultural residue– Cocos nucifera L.," *Biomass and Bioenergy* 46, 555-563. DOI: 10.1016/j.biombioe.2012.06.039

Malucelli, L., Lomonaco, D., Filho, M., and Magalhães, W. (2019). "Cellulose triacetate from different sources: modification assessment through thermal and chemical characterization," *Holzforschung* 74. DOI: 10.1515/hf-2019-0035

Matsumura, H., Sugiyama, J., and Glasser, W. (2000). "Cellulosic nanocomposites. I. Thermally deformable cellulose hexanoates from heterogeneous reaction," *Journal of Applied Polymer Science*. DOI: 10.1002/1097-4628(20001220)78:13%3C2242::AID-APP20%3E3.0.CO;2-5

Meereboer, K. W., Pal, A. K., Misra, M., and Mohanty, A. K. (2020). "Sustainable PHBV/cellulose acetate blends: Effect of a chain extender and a plasticizer," *ACS Omega* 5(24), 14221-14231. DOI: 10.1021/acsomega.9b03369

Morsy, A., Mahmoud, A. S., Soliman, A., Ibrahim, H., and Fadl, E. (2022). "Improved anti-biofouling resistances using novel nanocelluloses/cellulose acetate extracted from rice straw-based membranes for water desalination," *Scientific Reports* 12(1), 4386. DOI: 10.1038/s41598-022-08324-8

Motaung, T. E., and Linganiso, L. Z. (2018). "Critical review on agrowaste cellulose applications for biopolymers," *International Journal of Plastics Technology* 22(2), 185–216.

Nazir, N., Juita, E., Amelia, C., and Fatli, R. (2016). "Optimization of pre-treatment process of cocoa pod husk using various chemical solvents," *International Journal on Advanced Science, Engineering and Information Technology* 6(3), 403–409.

Nguyen, T. P. N., Yun, E.-T., Kim, I.-C., and Kwon, Y.-N. (2013). "Preparation of cellulose triacetate/cellulose acetate (CTA/CA)-based membranes for forward osmosis," *Journal of Membrane Science* 433, 49-59. DOI: 10.1016/j.memsci.2013.01.027

Ouattara, L. Y., Kouassi, E. K. A., Soro, D., Soro, Y., Yao, K. B., Adouby, K., Drogui, A. P., Tyagi, D. R., and Aina, P. M. (2021). "Cocoa pod husks as potential sources of renewable high-value-added products: A review of current valorizations and future prospects," *BioResources* 16(1), 1988-2020. DOI: 10.15376/biores.16.1.Ouattara

Pinto, E., Aggrey, W. N., Boakye, P., Amenuvor, G., Sokama-Neuyam, Y. A., Fokuo, M. K., Karimaie, H., Sarkodie, K., Adenutsi, C. D., Erzuah, S., and Rockson, M. A. D.

(2022). "Cellulose processing from biomass and its derivatization into carboxymethylcellulose: A review," *Scientific African* 15, article e01078. DOI: 10.1016/j.sciaf. 2021.e01078

Poletto, M., Pistor, V., Zeni, M., and Zattera, A. J. (2011). "Crystalline properties and decomposition kinetics of cellulose fibers in wood pulp obtained by two pulping processes," *Polymer Degradation and Stability* 96(4), 679-685. DOI: 10.1016/j.polymdegradstab.2010.12.007

Reddy, N., and Yang, Y. (2005). "Biofibers from agricultural byproducts for industrial applications," *TRENDS in Biotechnology* 23(1), 22-27.

Rodrigues Filho, G., da Cruz, S. F., Pasquini, D., Cerqueira, D. A., de Souza Prado, V., and de Assunção, R. M. N. (2000). "Water flux through cellulose triacetate films produced from heterogeneous acetylation of sugar cane bagasse," *Journal of Membrane Science* 177(1–2), 225-231.

Rodrigues Filho, G., Monteiro, D. S., Meireles, C. da S., de Assunção, R. M. N., Cerqueira, D. A., Barud, H. S., Ribeiro, S. J. L., and Messadeq, Y. (2008). "Synthesis and characterization of cellulose acetate produced from recycled newspaper," *Carbohydrate Polymers* 73(1), 74-82. DOI: 10.1016/j.carbpol.2007.11.010

Samios, E., Dart, R. K., and Dawkins, J. V. (1997). "Preparation, characterization and biodegradation studies on cellulose acetates with varying degrees of substitution," *Polymer* 38(12), 3045-3054. DOI: 10.1016/S0032-3861(96)00868-3

Samuel, O. S., and Adefusika, A. M. (2019). *Influence of Size Classifications on the Structural and Solid-State Characterization of Cellulose Materials*, *Cellulose*, IntechOpen. DOI: 10.5772/intechopen.82849

Sandesh, K., Shishir, R. K., and Vaman Rao, C. (2020). "Optimization and comparison of induction heating and LPG assisted acid pretreatment of cocoa pod for ABE fermentation," *Fuel* 262, article 116499. DOI: 10.1016/j.fuel.2019.116499

Sazali, N., Salleh, W. N. W., Ismail, A. F., Kadirgama, K., Othman, F. E. C., and Ismail, N. H. (2019). "Impact of stabilization environment and heating rates on P84 co-polyimide/nanocrystaline cellulose carbon membrane for hydrogen enrichment," *International Journal of Hydrogen Energy*, A Special Issue on Towards a Sustainable Hydrogen Production and Utilization, 44(37), 20924-20932. DOI: 10.1016/j.ijhydene.2018.06.039

Segal, L., Creely, J. J., Martin, A. E., and Conrad, C. M. (1959). "An empirical method for estimating the degree of crystallinity of native cellulose using the X-ray diffractometer," *Textile Research Journal* 29(10), 786-794. DOI: 10.1177/004051755902901003

Shaikh, H. M., Anis, A., Poulose, A. M., Al-Zahrani, S. M., Madhar, N. A., Alhamidi, A., Aldeligan, S. H., and Alsubaie, F. S. (2022). "Synthesis and characterization of cellulose triacetate obtained from date palm (*Phoenix dactylifera* L.) trunk mesh-derived cellulose," *Molecules* 27(4), article 1434. DOI: 10.3390/molecules27041434

Silva, F. B. da, Morais Júnior, W. G. de, Silva, C. V. da, Vieira, A. T., Batista, A. C. F., Faria, A. M. de, and Assunção, R. M. N. (2017). "Preparation and characterization of cellulose triacetate as support for lecitase ultra immobilization," *Molecules* 22(11), 1930. DOI: 10.3390/molecules22111930

Statista. (2022). *Cocoa beans: World Production by Country 2016-2022*.

Titiloye, J. O., Bakar, M. S. A., and Odetoye, T. E. (2013). "Thermochemical characterisation of agricultural wastes from West Africa," *Industrial Crops and Products* 47, 199-203.

To Nu, D., Hung, Hoang, and Bruggen, V. (2019). "Preparation of an asymmetric membrane from sugarcane bagasse using DMSO as green solvent," *Applied Sciences* 9, article 3347. DOI: 10.3390/app9163347

Tristantini Budi, D., and Yunan, A. (2018). "Advanced characterization of microbeads replacement from cellulose acetate based on empty fruit bunches and dried jackfruit leaves," *E3S Web of Conferences* 67, article 04045. DOI: 10.1051/e3sconf/20186704045

Tserki, V., Matzinos, P., Kokkou, S., and Panayiotou, C. (2005). "Novel biodegradable composites based on treated lignocellulosic waste flour as filler. Part I. Surface chemical modification and characterization of waste flour," *Composites Part A: Applied Science and Manufacturing* 36(7), 965-974.

Varghese, S. A., Pulikkalparambil, H., Rangappa, S. M., Siengchin, S., and Parameswaranpillai, J. (2020). "Novel biodegradable polymer films based on poly(3-hydroxybutyrate-co-3-hydroxyvalerate) and *Ceiba pentandra* natural fibers for packaging applications," *Food Packaging and Shelf Life* 25, article 100538. DOI: 10.1016/j.fpsl.2020.100538

Vroman, I., and Tighzert, L. (2009). "Biodegradable polymers," *Materials* 2(2), 307-344.

Wang, H., Zhang, X., Jiang, Z., Li, W., and Yu, Y. (2015). "A comparison study on the preparation of nanocellulose fibrils from fibers and parenchymal cells in bamboo (Phyllostachys pubescens)," *Industrial Crops and Products* 71, 80-88.

Yang, J., Kubota, F., Baba, Y., Kamiya, N., and Goto, M. (2014). "Application of cellulose acetate to the selective adsorption and recovery of Au (III)," *Carbohydrate Polymers* 111, 768-774. DOI: 10.1016/j.carbpol.2014.05.003